Letter | Editors' Suggestion | Featured in Physics

Ultrafast dynamics of chiral spin structures in synthetic antiferromagnets

Zongxia Guo,[1,2] Raphael Gruber,[3] Dmitriy Ksenzov,[4] Cyril Léveillé,[1,2] Matteo Pancaldi,[5,6] Emanuele Pedersoli,[5] Carlo Spezzani,[5] Giovanni De Ninno,[5,7] Flavio Capotondi,[5] Christian Gutt,[4] Mathias Kläui,[3] Vincent Cros,[2] Nicolas Reyren,[2] and Nicolas Jaouen[1,6]

[1]*Synchrotron SOLEIL, Saint-Aubin, Boite Postale 48, 91192 Gif-sur-Yvette Cedex, France*
[2]*Laboratoire Albert Fert, CNRS, Thales, Université Paris-Saclay, 91767 Palaiseau, France*
[3]*Institute of Physics, Johannes Gutenberg-Universität Mainz, Staudingerweg 7, 55128 Mainz, Germany*
[4]*Department Physik, Universität Siegen, Walter-Flex-Strasse 3, 57072 Siegen, Germany*
[5]*Elettra-Sincrotrone Trieste, 34149 Basovizza, Trieste, Italy*
[6]*Department of Molecular Sciences and Nanosystems, Ca' Foscari University of Venice, 30172 Venezia, Italy*
[7]*Laboratory of Quantum Optics, University of Nova Gorica, 5001 Nova Gorica, Slovenia*

(Received 3 March 2025; revised 16 May 2025; accepted 29 May 2025; published 28 July 2025)

In synthetic antiferromagnetic multilayers (SAFs), chiral magnetic structures such as spin spirals and skyrmions have been stabilized at room temperature by precisely tuning the effective perpendicular magnetic anisotropy, the Dzyaloshinskii-Moriya interaction, and the Ruderman-Kittel-Kasuya-Yoshida (RKKY) interlayer coupling. In this study, we investigate the dynamics of spin spirals on ultrashort timescales after femtosecond laser pumping in SAFs. The access to ultrafast magnetization dynamics, inaccessible by conventional optical techniques due to the zero net magnetization, has been enabled by the use of time-resolved circular dichroism in x-ray resonant magnetic scattering (CD-XRMS). A pair of two-dimensional x-ray scattering patterns for left and right elliptical polarization (EL and ER) have been recorded for each delay. In contrast to our previous findings in ferromagnetic multilayers, the magnetization (EL + ER) and dichroism (EL − ER) signals exhibit notably similar ultrafast dynamics, with demagnetization occurring on a timescale of ∼180 fs, followed by rapid remagnetization within ∼500 fs. This similarity in ultrafast dynamics can be attributed to the continuous rotation of magnetization in the spin spiral of SAFs, which evolves smoothly in space without forming abrupt domains or alternating domain walls. The ultrafast response and stability in its topological character highlight the potential of SAF-based chiral magnetic structures for future high-speed, energy-efficient data storage and processing applications.

DOI: 10.1103/1f11-n7dc

Chiral spin textures have gained considerable attention in recent years following the discovery of the interfacial Dzyaloshinskii-Moriya interaction (DMI) [1,2]. Such interfacial DMI, a form of antisymmetric exchange interaction, favors a preferred chirality for spin textures and plays a pivotal role in the formation of skyrmions in nanoscale thin-film, which paves the way for potential high-density data storage and in-memory computing applications [3–7]. However, skyrmions in ferromagnets exhibit several limitations that hinder their potential use in functional devices. These include their dependence on nonlocal stray fields for stabilization, resulting in minimal skyrmion sizes of several tens of nanometers at room temperature, and the necessity for an external magnetic field for their stabilization [8–11]. Moreover, the skyrmion Hall effect, arising from the finite topological charge, induces a deflection in their motion along tracks, which can potentially result in annihilation at track edges [12–14].

Synthetic antiferromagnets (SAFs), consisting of periodically separated ferromagnetic (FM) layers coupled antiferromagnetically through a nonmagnetic spacer via the Ruderman-Kittel-Kasuya-Yoshida (RKKY) interaction, exhibit minimal stray fields and rapid magnetization precession relative to FM systems [15,16]. Skyrmions in SAFs, formed by two skyrmions with antiparallel spins, offer numerous advantages over their ferromagnetic counterparts [17,18]. First, their vanishing magnetization allows for room-temperature stability and diameters of tens of nanometers without the need for external fields [19]. Their zero net topological charge eliminates the skyrmion Hall effect, enabling a straight trajectory along the current with velocities near 1000 m/s and enhanced the thermal skyrmion diffusion [20–22]. Additionally, their zero net magnetization renders them immune to external magnetic fields, though this feature makes such magnetic structure detection more challenging.

Recent advancements in soft x-ray resonant magnetic scattering (XRMS), with element selectivity, three-dimensional (3D) spatial-resolved sensitivity, and imaging techniques using coherence properties of modern light sources, have opened new possibilities for the study of magnetic multilayers [23–25]. XRMS has recently enabled direct access to key features such as domain-wall types (Néel or Bloch), and the chirality (clockwise or counterclockwise) of spin textures [26]. In our previous work [27], the SAF multilayers with a multilayer period of 2.15 nm, two separate (in Q) peaks appear for the structural and the magnetic periodicities emerge in resonant reflectivity measurements when the x-ray wavelength is tuned to the core-level L (or K) edges of the magnetic element

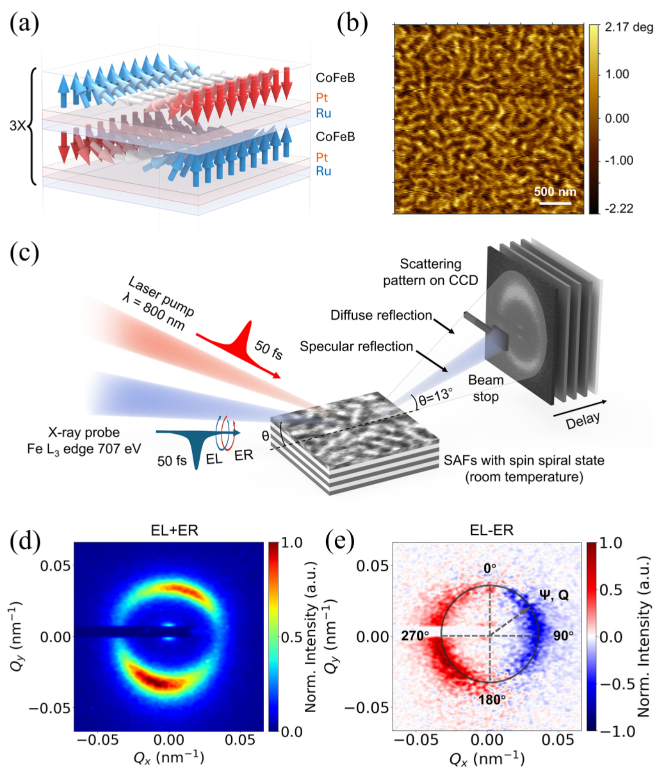

FIG. 1. Sample description and experimental geometry. (a) Sketch of the SAF multilayer stack. (b) The MFM phase map image displays labyrinthine domains with a magnetic period of ∼190 nm after out-of-plane field demagnetization. (c) Experimental configuration with the incident beams of the linearly polarized infrared laser pump and the elliptically polarized x-ray probe. A typical static (d) sum (EL + ER) and (e) difference (EL − ER) scattering pattern.

[28,29]. We showed that the chirality of our SAF sample remain stable across a broad temperature range, suggesting similar temperature dependencies for both the exchange stiffness and the DMI [27,30].

In this study, we investigate the behavior of these chiral magnetic textures in SAFs at an ultrashort timescale. The complete SAF stack is Ta (5 nm)/Pt (8 nm)/[$Co_{0.4}Fe_{0.4}B_{0.2}$ (0.9 nm)/Ru (0.75 nm)/Pt (0.5 nm)$]_{\times 6}$/Al (5 nm), as illustrated in Fig. 1(a). This multilayer structure is deposited at room temperature by magnetron sputtering onto a thermally oxidized silicon wafer. Each pair of adjacent CoFeB ferromagnetic layers is antiferromagnetically coupled through the Ru spacer with an optimized thickness [19]. In addition, our multilayered sample is engineered with the DMI that enforces a Néel texture and a near-zero effective anisotropy, thereby stabilizing Néel type (cycloidal) spin spirals in each CoFeB layers. After demagnetization by an out-of-plane magnetic field, the MFM phase map reveals labyrinth domains, as shown in Fig. 1(b). However, the stray field from the SAF is orders of magnitude smaller than in an FM, so the MFM image is acquired in vacuum to increase the sensitivity of the measurement.

The time-resolved experiments are carried out taking advantage of the recent possibility of the FERMI free-electron laser (FEL) light source to deliver a high flux of elliptical polarized x rays (∼43% of circular polarization) up to Fe L_3-edges (707 eV) as described in [32]. In the pump-probe experiment, a 795-nm wavelength infrared (IR) pump laser (300 × 300 μm^2 spot size) and x-ray probe (250 × 250 μm^2 spot size) with both 50 fs (FWHM) pulse duration have been synchronized and spatially aligned in the DiProI beamline of FERMI [33]. The experimental setup for the scattering experiment is shown schematically in Fig. 1(c). To establish resonant scattering conditions in SAFs, the FEL-2 line uses nonlinear harmonic generation to reach the Fe L_3-edge, which exhibits magnetic scattering contrast arising from the x-ray magnetic circular dichroism (XMCD) effect. Due to the strong ferromagnetic exchange coupling between Fe and Co moments, the Fe sublattice dynamics reflect the magnetic behavior of the CoFeB layer. The diffuse scattering pattern is detected on a two-dimensional (2D) charge-coupled device (CCD) detector. Figures 1(d) and 1(e) show the static

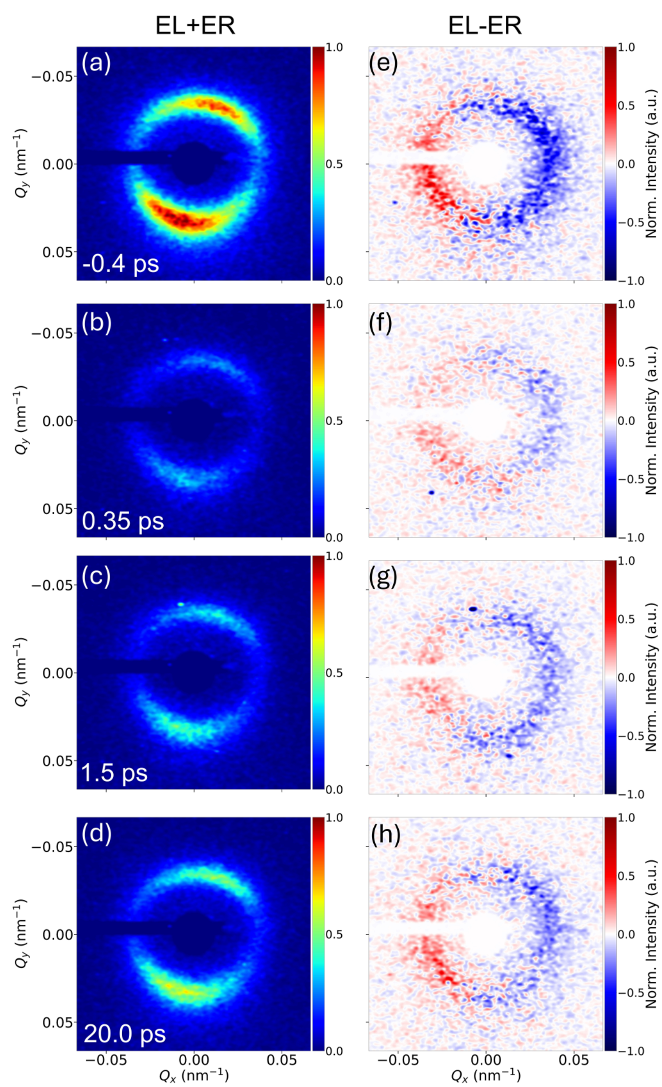

FIG. 2. Scattering pattern evolution with delay time. Scattering patterns for the sum (a)–(d) EL + ER and (e)–(h) the difference EL − ER images for the initial, +0.35 ps, +1.5 ps, and +20 ps states. Gaussian filtering was applied to all images to improve visualization.

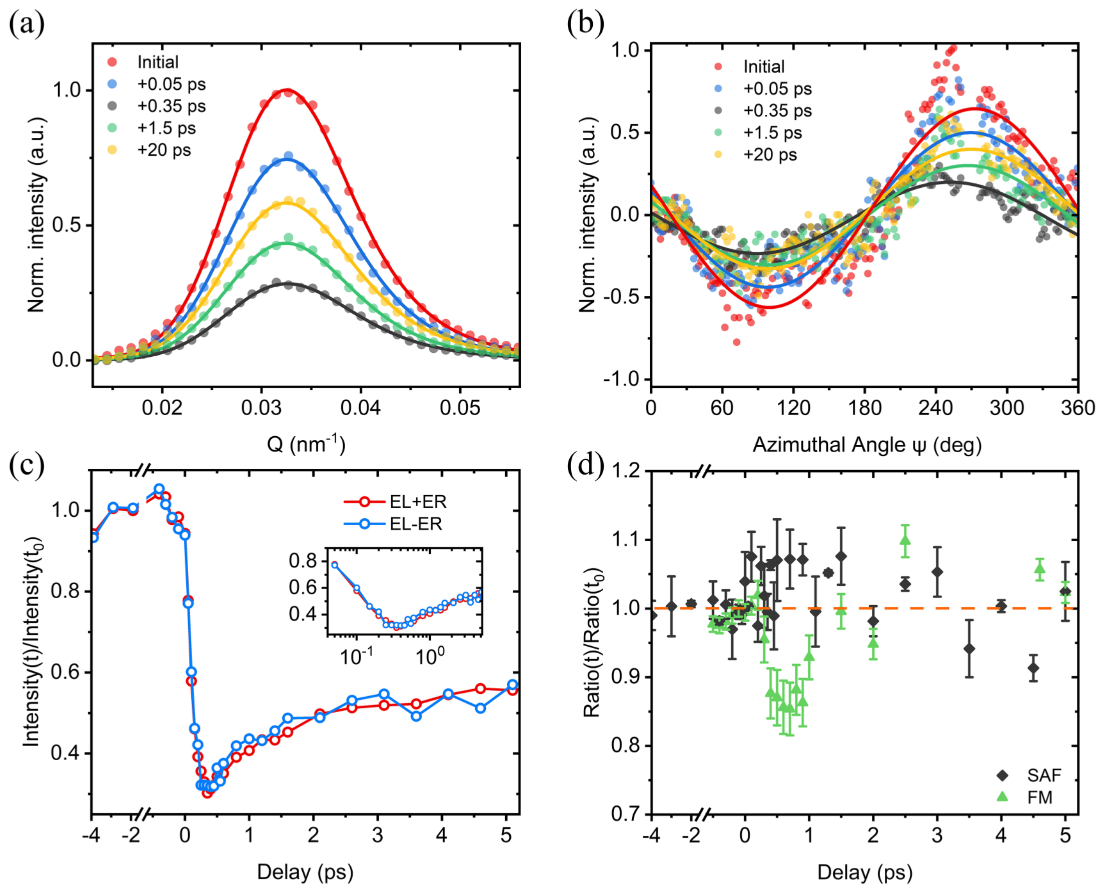

FIG. 3. Evolution of the time-resolved XRMS signal during the first 5 ps. (a) The radial profiles of the sum EL + ER. (b) The orthoradial dichroic profiles (EL − ER). (c) The intensity of integrated scattering rings (EL + ER) and dichroism (EL − ER) is normalized to their values during negative time delays. The insert shows the time delay in log scale. (d) The asymmetry ratio (EL − ER)/(EL + ER) is analyzed over the first 5 ps (black diamonds). In contrast to the chiral FM multilayers (green triangles) studied by Léveillé *et al.* [31], which exhibit an asymmetry ratio below unity within 2 ps, the SAF maintains a constant ratio close to 1. The error bar is determined from signal background processing and fitting errors.

magnetic scattering patterns, which have a ring shape related to a spin spiral period of ∼190 nm. These patterns can only be observed in $Q_{\mathrm{Bragg}}/2$ or odd multiple incident angle position due to the antiparallel period multilayer structure [27]. From the orthoradial profile of the difference pattern [Fig. 1(e)], we confirm that the counterclockwise (CCW) Néel type magnetic textures are stabilized as expected [26]. Pumped by the IR laser with a fluence of 5.2 mJ/cm^2, a series of scattering patterns using elliptical left and right (EL and ER) x-ray probes is acquired. The scattering patterns of the sum (EL + ER) and the dichroic (EL − ER) signal at selected time delays are shown in Fig. 2. At +0.35 ps [Figs. 2(b) and 2(f)], the intensity of both signals has significantly decreased compared to their initial states [Figs. 2(a) and 2(e)], followed by a noticeable partial recovery in both signals thereafter [Figs. 2(c), 2(g), 2(d), and 2(h)].

The sum signal is analyzed by integrating the radial profile, removing the background, and fitting it with a Gaussian function [31,34,35], showing a strong decrease in amplitude after IR pumping, as shown in Fig. 3(a). The orthoradial profile is fitted with the sine function within the exchanged momentum interval 0.02 to 0.05 nm^{-1} of the dichroic signal, as shown in Fig. 3(b). Figure 3(c) compares the magnetic and chiral order dynamics in the SAFs, where the sum (EL + ER) derived from the Gaussian fit amplitude (red curve) and the difference (EL − ER) obtained from the sine fit amplitude (blue curve). These curves exhibit a typical signature of ultrafast demagnetization in our multilayer sample: an initial quenching of the magnetization to a minimum value within a few hundred femtoseconds, followed by a rapid recovery over several picoseconds. In Fig. 3(d), we show the normalized asymmetry ratio (EL − ER)/(EL + ER) as a function of time. It is important to note that this ratio remains close to unity, indicating that the ultrafast dynamics of both magnetization and chirality remain essentially the same at an ultrafast timescale. Compared to the results reported by Léveillé *et al.* [31] for Co/Pt FM multilayers with chiral spin structures [green triangles in Fig. 3(d)], which exhibit an asymmetry ratio below unity within 2 ps, SAFs exhibit no discernible difference between the dynamics of magnetization and dichroism, given the limitations of the signal-to-noise ratio. This can be explained by the absence of well-defined magnetic domains and domain walls in the spin spiral structure [26,31]. So, under the ultrafast demagnetization mechanism driven by hot electrons, both dichroism and magnetization signals display the same ultrafast behavior.

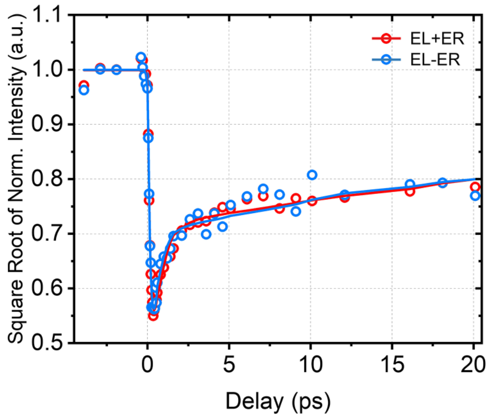

FIG. 4. Ultrafast demagnetization of scattering intensity, calculated as the square root of the measured intensity [Fig. 3(c)], fitted to the three-temperature model within the range of −5 ps to +20 ps.

Considering the quadratic relationship between magnetic x-ray scattering intensity and magnetization [35], the characteristic timescales were extracted by fitting the square root of the intensity using the three-temperature model [36], which describes the intensity as the convolution of exponential functions with a Gaussian function associated with the FEL time resolution, as shown below:

$$\frac{\Delta M}{M(0)} = \left[1 + \left(\frac{-A_1}{\sqrt{\Delta t/\tau_0 + 1}} + \frac{(A_2\tau_E - A_1\tau_M)}{\tau_E - \tau_M} e^{-\Delta t/\tau_M} + \frac{\tau_E(A_1 - A_2)}{\tau_E - \tau_M} e^{-\Delta t/\tau_E}\right)\theta(\Delta t)\right] \otimes \Gamma(\Delta t). \quad (1)$$

The $M(0)$ is the initial magnetization level; A_1 is the amplitude of the partial recovery after the electrons, spins, and lattice have reached thermal equilibrium; A_2 is proportional to the initial electron temperature rise, describing the initial magnetization quenching; τ_M is the time constant of demagnetization; τ_E is the electron-phonon relaxation time, characterizing the fast recovery of magnetization; and τ_0 is a characteristic time describing cooling by heat diffusion. $\theta(\Delta t)$ and $\Gamma(\Delta t)$ stand for a Heaviside and a Gaussian function. The latter mimics the limited experimental time resolution due to the finite length of the x-ray and IR pulses. Here, the time resolution is $\sqrt{\sigma_{\mathrm{IR}}^2 + \sigma_{\mathrm{FEL}}^2} \approx 71$ fs. As shown in Fig. 4, after the ultrafast quenching reaches a maximum of around 350 fs, the ultrafast recovery takes place in the next few ps. Both the sum and difference signals exhibit a demagnetization time of 180 ± 5 fs and a recovery time of 500 ± 20 fs.

The ultrafast dynamics in spin spiral SAFs differ significantly from those in FM multilayers. In Co/Pt multilayer FM chiral systems, the demagnetization time is 390 ± 100 fs, and the fast recovery time is around 2000 ± 1000 fs [34,35]. In contrast, SAFs exhibit faster timescales. Accounting for the negligible influence of different magnetic textures on the characteristic timescale of ultrafast dynamics as shown in [37,38], we can therefore attribute, in agreement with [39], this faster timescale to the antiferromagnetic coupling of sublattices in SAFs, leading to accelerated spin dynamics and increased spin scattering and transport processes, which enhance demagnetization.

In summary, our time-resolved XRMS experiments on spin spiral SAF multilayers have uncovered ultrafast dynamics that are notably different from those in ferromagnetic multilayers. By employing a linearly polarized IR pump and an elliptically polarized x-ray probe, we captured 2D x-ray scattering patterns and analyzed both the sum (EL + ER) and difference (EL − ER) signals to trace the evolution of magnetization and chirality at subpicosecond timescales. The SAF multilayers demonstrated a rapid demagnetization time of approximately 180 fs, followed by a recovery of approximately 500 fs, which is significantly faster than FM. The consistency of the ultrafast dynamics in both magnetization and chirality signals supports a demagnetization mechanism driven by hot electrons.

We thank J.Y. Chauleau and M. Viret for fruitful discussions. Financial support by the Agence Nationale de la Recherche, France, under Grant Agreement No. ANR-20-CE42-0012 (MEDYNA), by France 2030 government investment plan managed by the French National Research Agency under Grants No. PEPR SPIN-CHIREX ANR-22-EXSP-0002 and No. SPIN-CHARAC ANR-22-EXSP-0008 from a joint DFG-ANR 22 grant (TOPO3D) is acknowledged. D.K. and C.G. acknowledge funding by the Deutsche Forschungsgemeinschaft (DFG) Projects No. GU 535/9-1 and No. KS 62/3-1. C.G. acknowledges funding from BMBF(05K24PSA) and DFG (NFDI 40/1). M.K. and R.G. acknowledge funding by the DFG (No. 423441604 and SFB TRR 173 Spin+X, A01, A12, B02, No. 268565370), the European Commission (ERC-2019-SyG, No. 856538 3D MAGiC) and the Horizon Europe Project No. 101070290 (NIMFEIA). We thank the FERMI free-electron laser facility for the beam time allocated under Proposal No. 20214047.

The data that support the findings of this article are not publicly available. The data are available from the authors upon reasonable request.

[1] A. Thiaville, S. Rohart, É. Jué, V. Cros, and A. Fert, Dynamics of Dzyaloshinskii domain walls in ultrathin magnetic films, Europhys. Lett. **100**, 57002 (2012).

[2] M. Kuepferling, A. Casiraghi, G. Soares, G. Durin, F. Garcia-Sanchez, L. Chen, C. H. Back, C. H. Marrows, S. Tacchi, and G. Carlotti, Measuring interfacial Dzyaloshinskii-Moriya interaction in ultrathin magnetic films, Rev. Mod. Phys. **95**, 015003 (2023).

[3] A. Fert, V. Cros, and J. Sampaio, Skyrmions on the track, Nat. Nanotechnol. **8**, 152 (2013).

[4] A. Fert, N. Reyren, and V. Cros, Magnetic skyrmions: advances in physics and potential applications, Nat. Rev. Mater. **2**, 17031 (2017).

[5] K. Everschor-Sitte, J. Masell, R. M. Reeve, and M. Kläui, Perspective: Magnetic skyrmions—Overview of recent progress in an active research field, J. Appl. Phys. **124**, 240901 (2018).

[6] G. Finocchio, F. Büttner, R. Tomasello, M. Carpentieri, and M. Kläui, Magnetic skyrmions: from fundamental to applications, J. Phys. D **49**, 423001 (2016).

[7] D. Prychynenko, M. Sitte, K. Litzius, B. Krüger, G. Bourianoff, M. Kläui, J. Sinova, and K. Everschor-Sitte, Magnetic skyrmion as a nonlinear resistive element: A potential building block for reservoir computing, Phys. Rev. Appl. **9**, 014034 (2018).

[8] S. Woo, K. Litzius, B. Krüger, M.-Y. Im, L. Caretta, K. Richter, M. Mann, A. Krone, R. M. Reeve, M. Weigand *et al.*, Observation of room-temperature magnetic skyrmions and their current-driven dynamics in ultrathin metallic ferromagnets, Nat. Mater. **15**, 501 (2016).

[9] F. Büttner, I. Lemesh, and G. S. Beach, Theory of isolated magnetic skyrmions: From fundamentals to room temperature applications, Sci. Rep. **8**, 4464 (2018).

[10] C. Moreau-Luchaire, C. Moutafis, N. Reyren, J. Sampaio, C. Vaz, N. Van Horne, K. Bouzehouane, K. Garcia, C. Deranlot, P. Warnicke *et al.*, Additive interfacial chiral interaction in multilayers for stabilization of small individual skyrmions at room temperature, Nat. Nanotechnol. **11**, 444 (2016).

[11] O. Boulle, J. Vogel, H. Yang, S. Pizzini, D. de Souza Chaves, A. Locatelli, T. O. Menteş, A. Sala, L. D. Buda-Prejbeanu, O. Klein *et al.*, Room-temperature chiral magnetic skyrmions in ultrathin magnetic nanostructures, Nat. Nanotechnol. **11**, 449 (2016).

[12] W. Jiang, X. Zhang, G. Yu, W. Zhang, X. Wang, M. Benjamin Jungfleisch, J. E. Pearson, X. Cheng, O. Heinonen, K. L. Wang *et al.*, Direct observation of the skyrmion Hall effect, Nat. Phys. **13**, 162 (2017).

[13] K. Litzius, I. Lemesh, B. Krüger, P. Bassirian, L. Caretta, K. Richter, F. Büttner, K. Sato, O. A. Tretiakov, J. Förster *et al.*, Skyrmion Hall effect revealed by direct time-resolved x-ray microscopy, Nat. Phys. **13**, 170 (2017).

[14] K. Litzius, J. Leliaert, P. Bassirian, D. Rodrigues, S. Kromin, I. Lemesh, J. Zazvorka, K.-J. Lee, J. Mulkers, N. Kerber *et al.*, The role of temperature and drive current in skyrmion dynamics, Nature Electronics **3**, 30 (2020).

[15] R. Duine, K.-J. Lee, S. S. Parkin, and M. D. Stiles, Synthetic antiferromagnetic spintronics, Nat. Phys. **14**, 217 (2018).

[16] V. Baltz, A. Manchon, M. Tsoi, T. Moriyama, T. Ono, and Y. Tserkovnyak, Antiferromagnetic spintronics, Rev. Mod. Phys. **90**, 015005 (2018).

[17] K. Wang, V. Bheemarasetty, and G. Xiao, Spin textures in synthetic antiferromagnets: Challenges, opportunities, and future directions, APL Mater. **11**, 070902 (2023).

[18] X. Zhang, Y. Zhou, and M. Ezawa, Antiferromagnetic skyrmion: stability, creation and manipulation, Sci. Rep. **6**, 24795 (2016).

[19] W. Legrand, D. Maccariello, F. Ajejas, S. Collin, A. Vecchiola, K. Bouzehouane, N. Reyren, V. Cros, and A. Fert, Room-temperature stabilization of antiferromagnetic skyrmions in synthetic antiferromagnets, Nat. Mater. **19**, 34 (2020).

[20] V. T. Pham, N. Sisodia, I. Di Manici, J. Urrestarazu-Larrañaga, K. Bairagi, J. Pelloux-Prayer, R. Guedas, L. D. Buda-Prejbeanu, S. Auffret, A. Locatelli *et al.*, Fast current-induced skyrmion motion in synthetic antiferromagnets, Science **384**, 307 (2024).

[21] S. Panigrahy, S. Mallick, J. Sampaio, and S. Rohart, Skyrmion inertia in synthetic antiferromagnets, Phys. Rev. B **106**, 144405 (2022).

[22] T. Dohi, M. Weißenhofer, N. Kerber, F. Kammerbauer, Y. Ge, K. Raab, J. Zázvorka, M.-A. Syskaki, A. Shahee, M. Ruhwedel *et al.*, Enhanced thermally-activated skyrmion diffusion with tunable effective gyrotropic force, Nat. Commun. **14**, 5424 (2023).

[23] E. Burgos-Parra, Y. Sassi, W. Legrand, F. Ajejas, C. Léveillé, P. Gargiani, M. Valvidares, N. Reyren, V. Cros, N. Jaouen *et al.*, Probing of three-dimensional spin textures in multilayers by field dependent x-ray resonant magnetic scattering, Sci. Rep. **13**, 11711 (2023).

[24] G. van der Laan and A. I. Figueroa, X-ray magnetic circular dichroism–A versatile tool to study magnetism, Coord. Chem. Rev. **277-278**, 95 (2014).

[25] M. Sacchi, N. Jaouen, H. Popescu, R. Gaudemer, J. M. Tonnerre, S. G. Chiuzbaian, C. F. Hague, A. Delmotte, J. M. Dubuisson, G. Cauchon, B. Lagarde, and F. Polack, The SEXTANTS beamline at SOLEIL: A new facility for elastic, inelastic and coherent scattering of soft x-rays, J. Phys.: Conf. Ser. **425**, 072018 (2013).

[26] J.-Y. Chauleau, W. Legrand, N. Reyren, D. Maccariello, S. Collin, H. Popescu, K. Bouzehouane, V. Cros, N. Jaouen, and A. Fert, Chirality in magnetic multilayers probed by the Symmetry and the amplitude of dichroism in x-ray resonant magnetic scattering, Phys. Rev. Lett. **120**, 037202 (2018).

[27] C. Léveillé, S. Flewett, E. Burgos-Parra, Y. Sassi, W. Legrand, F. Ajejas, V. Cros, N. Reyren, and N. Jaouen, Chiral spin spiral in synthetic antiferromagnets probed by circular dichroism in x-ray resonant magnetic scattering, Phys. Rev. B **104**, L060402 (2021).

[28] J. M. Tonnerre, L. Séve, D. Raoux, G. Soullié, B. Rodmacq, and P. Wolfers, Soft x-ray resonant magnetic scattering from a magnetically coupled Ag/Ni multilayer, Phys. Rev. Lett. **75**, 740 (1995).

[29] C. Spezzani, P. Torelli, M. Sacchi, R. Delaunay, C. F. Hague, A. Mirone, F. Salmassi, E. M. Gullikson, and J. H. Underwood, Magnetic coupling in Co/Cu multilayers: Field-dependent antiferromagnetic ordering investigated by resonant x-ray scattering, Surf. Rev. Lett. **09**, 921 (2002).

[30] K. Alshammari, E. Haltz, M. Alyami, M. Ali, P. S. Keatley, C. H. Marrows, J. Barker, and T. A. Moore, Scaling of Dzyaloshinskii-Moriya interaction with magnetization in Pt/Co (Fe) B/Ir multilayers, Phys. Rev. B **104**, 224402 (2021).

[31] C. Léveillé, E. Burgos-Parra, Y. Sassi, F. Ajejas, V. Chardonnet, E. Pedersoli, F. Capotondi, G. De Ninno, F. Maccherozzi, S. Dhesi *et al.*, Ultrafast time-evolution of chiral Néel magnetic domain walls probed by circular dichroism in x-ray resonant magnetic scattering, Nat. Commun. **13**, 1412 (2022).

[32] C. Spezzani, A. Ravindran, E. Allaria, L. Badano, R. Bhardwaj, A. Brynes, P. Capaldo, A. Caretta, P. Cinquegrana, A. Contillo *et al.*, Circular dichroism experiments at the L edge of magnetic transition metals enabled by elliptically polarized pulses from a seeded free-electron laser, Phys. Rev. B **110**, 174409 (2024).

[33] E. Pedersoli, F. Capotondi, D. Cocco, M. Zangrando, B. Kaulich, R. H. Menk, A. Locatelli, T. O. Mentes, C. Spezzani, G. Sandrin *et al.*, Multipurpose modular experimental station for the DiProI beamline of Fermi@ Elettra free electron laser, Rev. Sci. Instrum. **82**, 043711 (2011).

[34] N. Kerber, D. Ksenzov, F. Freimuth, F. Capotondi, E. Pedersoli, I. Lopez-Quintas, B. Seng, J. Cramer, K. Litzius, D. Lacour

et al., Faster chiral versus collinear magnetic order recovery after optical excitation revealed by femtosecond XUV scattering, Nat. Commun. **11**, 6304 (2020).

[35] C. Léveillé, Magnetization dynamics in chiral thin films probed by x-ray resonant magnetic resonant scattering, Ph.D. Thesis, Université Paris-Saclay, 2022.

[36] G. Malinowski, F. Dalla Longa, J. Rietjens, P. Paluskar, R. Huijink, H. Swagten, and B. Koopmans, Control of speed and efficiency of ultrafast demagnetization by direct transfer of spin angular momentum, Nat. Phys. **4**, 855 (2008).

[37] N. Zhou Hagström, R. Jangid, M. Madhavi, D. Turenne, J. A. Brock, E. S. Lamb, B. Stoychev, J. Schlappa, N. Gerasimova, B. Van Kuiken *et al.*, Symmetry-dependent ultrafast manipulation of nanoscale magnetic domains, Phys. Rev. B **106**, 224424 (2022).

[38] N. Moisan, G. Malinowski, J. Mauchain, M. Hehn, B. Vodungbo, J. Lüning, S. Mangin, E. Fullerton, and A. Thiaville, Investigating the role of superdiffusive currents in laser induced demagnetization of ferromagnets with nanoscale magnetic domains, Sci. Rep. **4**, 4658 (2014).

[39] A. De, S. S. P. K. Arekapudi, L. Koch, F. Samad, S. N. Panda, B. Böhm, O. Hellwig, and A. Barman, Magnetic configuration driven femtosecond spin dynamics in synthetic antiferromagnets, ACS Appl. Mater. Interfaces **14**, 13970 (2022).